

Received: 2018.12.02  
Accepted: 2019.02.20  
Published: 2019.07.10

# Long-Chain Non-Coding RNA (lncRNA) MT1JP Suppresses Biological Activities of Lung Cancer by Regulating miRNA-423-3p/Bim Axis

Authors' Contribution:  
Study Design A  
Data Collection B  
Statistical Analysis C  
Data Interpretation D  
Manuscript Preparation E  
Literature Search F  
Funds Collection G

ABC **Jiyong Ma**  
BCD **Haijun Yan**  
CDE **Jing Zhang**  
DEF **Yan Tan**  
EFG **Wei Gu**

Department of Respiration, Nanjing First Hospital, Nanjing Medical University, Nanjing, Jiangsu, P.R. China

**Corresponding Author:** Wei Gu, e-mail: [guwei0112@163.com](mailto:guwei0112@163.com)

**Source of support:** This study was supported by the Nanjing Medical Science and Technology Development Project (YKK15084)

**Background:** This study aimed to explain the effects and mechanism of MT1JP in lung cancer development and treatment.





**Material/Methods:** Thirty non-small cell lung cancer (NSCLC) (stages I–II, 17 cases; stages III–IV, 13 cases) and adjacent normal tissues were obtained. MT1JP and miRNA-423-3p levels were assessed by *in situ* hybridization and Bim protein expression by immunohistochemistry, and the correlations determined were analyzed. Cell proliferation was determined using MTT and colony formation assay, and cell apoptosis was measured using flow cytometry. A549 cell invasion and migration were assessed by Transwell migration and scratch wound healing assays. Relative mRNA and protein expressions were assessed using real-time polymerase chain reaction and western blotting. Correlations between miRNA-423-3p and Bim protein were investigated using luciferase activity assay, and Bim protein expression was evaluated using western blotting.

**Results:** MT1JP, miRNA-423-3p, and Bim expressions in NSCLC cancer tissues and those in adjacent cancer tissues were significantly different ( $P < 0.01$  or  $P < 0.001$ ) with increasing stage. Compared with those in the normal control (NC) group, cell proliferation rates were significantly suppressed ( $P < 0.01$  or  $P < 0.001$ ) and cell apoptosis rates significantly increased ( $P < 0.01$  or  $P < 0.001$ ) in the miRNA inhibitor and lncRNA+miRNA inhibitor groups. Invasion cell numbers and wound healing rates were also significantly inhibited in the miRNA inhibitor and lncRNA+miRNA inhibitor groups ( $P < 0.01$  or  $P < 0.001$ ) compared with those in the NC group.

**Conclusions:** The lncRNA MT1JP suppresses NSCLC biological activities by regulating the miRNA-423-3p/Bim axis.

**MeSH Keywords:** **Ankle Fractures • Carcinoma, Non-Small-Cell Lung • MicroRNAs • RNA, Long Noncoding**

**Full-text PDF:** <https://www.medscimonit.com/abstract/index/idArt/914387>

 3835  —  7  30



## Background

Due to changes in lifestyle and increased environmental pollution, lung cancer has become one of the fastest-growing malignant tumors worldwide with high morbidity and mortality. As such, this type of cancer presents a serious threat to human life and health. The incidence of lung cancer in China has significantly increased in recent years. Studies show that smoking, environmental pollution, and chronic obstructive pulmonary diseases are all risk factors for lung cancer [1,2]. Non-small cell lung cancer (NSCLC) accounts for approximately 80% of all lung cancer cases [3]. While surgery is currently the most effective treatment for this type of cancer, a diagnosis is not established in approximately 70% of patients with lung cancer until the disease reaches an advanced stage; at such a stage surgery is no longer an option. Despite adopting radiotherapy, chemotherapy, and molecular targeted therapy, the 5-year survival of these patients remains low. Therefore, effective therapeutic targets for treating NSCLC and highly effective and low-toxicity drugs are warranted.

Bim is a member of the Bcl-2 family, which comprises important death-decision makers in the process of apoptosis. The human Bim gene is located at 2q12-q13 of the human genome. The deficiency of the Bim gene is an important factor that is correlated with the increased malignancy of lung cancer [4–7].

Long-chain non-coding RNAs (lncRNAs) are a class of non-coding RNAs that are over 200 bp in length and are ubiquitous in mammals. They have a wide range of biological functions, such as regulating gene transcription and translation, protein localization, cell structural integrity, cell cycle, and inflammatory response [8]. The expression of the lncRNA MT1JP, which is abundant in normal tissues, is reduced in lung, liver, colorectal, and gastric cancer tissues [9–11]. Recent studies have confirmed that lncRNAs can regulate protein expression through related single-stranded non-coding small RNAs (miRNAs) [12,13]. miRNAs are widely found in plants and animals and are approximately 22 nucleotides in length; these molecules bind to the 3'-untranslated region (UTR) of perfectly or partially complementary target mRNAs, leading to the degradation of mRNA or inhibition of mRNA translation [14–16]. Pathophysiological findings suggest that miRNAs are involved in a variety of biological processes, and recent studies confirm that miRNA-423-3p can target Bim to enhance tumor cell activity [17]. However, whether MT1JP inhibits lung cancer activity by downregulating miRNA-423-3p and, consequently, upregulating Bim is unknown. In this study, we first detected the expressions of MT1JP, miRNA-423-3p, and Bim protein in lung cancer tissues at different stages of the disease, as well as para-cancerous tissues, by either *in situ* hybridization (ISH) or immunohistochemistry (IHC) and analyzed their correlations; subsequently, through *in vitro* cellular experiments, we

investigated the mechanism through which MT1JP inhibits the biological activity of the NSCLC A549 cell line.

## Material and Methods

### Clinical information

Thirty patients with NSCLC who were admitted to the Department of Respiratory Medicine of the First Hospital of Nanjing from September 2013 to August 2015 were enrolled in this study, including 17 patients at stages I–II and 13 patients at stages III–IV. None of NSCLC patients received any treatment before their operation. All patients were primary NSCLC. The resected lung cancer and adjacent normal tissues were fixed in 10% paraformaldehyde for 24 hours.

### Hematoxylin and eosin staining

The samples were rinsed sequentially in tap water, 75% ethanol, 85% ethanol, 95% ethanol I, 95% ethanol II, absolute ethanol/chloroform (1: 1), and chloroform I for 1 hour in each solvent and then in chloroform II overnight, in chloroform/paraffin (1: 1) for 40 minutes, in paraffin I for 1 hour, in paraffin II for 1 hour, and in paraffin III for 30 minutes. A small amount of wax was poured onto the bottom of an embedding mold, the tissue was taken out and placed on top of this wax, and then additional wax was slowly poured into the mold until it was completely filled. Thereafter, the mold was allowed to cool and solidify. The wax block was trimmed and stored at 4°C. Four-micrometer sections were made and dehydrated in xylene I for 30 min, xylene II for 30 minutes, 100% ethanol I for 5 minutes, 100% ethanol II for 5 minutes, 95% ethanol for 5 minutes, 90% ethanol for 5 minutes, 80% ethanol for 5 minutes, and distilled water twice. The sections were stained with Mayer's hematoxylin staining solution for 3–10 minutes, rinsed with tap water for 5 minutes and distilled water for 2 minutes, and then counterstained with eosin dye solution for 5 minutes; rinsing with tap water for 5 minutes followed. The sections were soaked in 80% ethanol for 2 minutes, 90% ethanol for 2 minutes, 95% ethanol for 2 minutes, 100% ethanol I for 5 minutes, 100% ethanol II for 5 minutes, xylene for I for 5 minutes, and then xylene II for 5 minutes for dehydration and transparency. Finally, the sections were sealed with a drop of neutral resin before the xylene dried out and observed under an optical microscope.

### In situ hybridization

The experimental procedures applied to detect miRNA-423-3p and lncRNA MT1JP were carried out as instructed by the manual provided by Wuhan Boster Biotech Co., Ltd., Wuhan, China. The slides were sterilized at 180°C for 6 hours and treated with

poly-lysine or triethoxysilane and distilled water; vessels were treated with diethylprocarbonate. The samples were fixed with 10% neutral formaldehyde for 20 hours, a paraffin-embedded tissue block was prepared, and sections with a thickness of 6–8  $\mu\text{m}$  were made. The paraffin sections were attached to the poly-L-lysine-coated slides and baked at 65°C for 45 minutes to ensure firm adherence to the slides. The paraffin sections were routinely dewaxed in water and then treated with 3%  $\text{H}_2\text{O}_2$  at room temperature for 5–10 minutes to inactivate endogenous enzymes. The sections were washed thrice with RNase-free water for 1 minute each time to expose the mRNA fragments, washed thrice with phosphate buffer saline (PBS) for 5 minutes, and then washed once more with RNase-free water for 1 minute before hybridization. The staining effect was observed under a microscope (B203LED; Aote, Chongqing, China).

### Immunohistochemistry

Conventional dehydration with gradient concentrations of ethanol and paraffin embedding were performed as described in previous literature. DAP (3,3'-diaminobenzidine) staining was performed according to the instructions of the kit, followed by hematoxylin counterstaining. The samples were rinsed in 1% hydrochloric acid–ethanol differentiation solution and warm water for “bluing up,” dehydrated with serial concentrations of ethanol, and sealed with neutral resin. The tissue sections were observed under an optical microscope with a 400 $\times$  lens. Images were taken from 5 fields with obvious Bim staining. Quantitative analysis was performed using Image-Pro Plus software to determine the integrated optical density values of each target.

### Cell culture and treatment

A549 cells were cultured in Dulbecco's Modified Eagle Medium (DMEM) supplemented with 10% fetal bovine serum (FBS), 100 U/mL penicillin, and 100  $\mu\text{g}/\text{mL}$  streptomycin and cultured in an incubator at 37°C with 5%  $\text{CO}_2$ . For passage, the cells were digested with 0.25% trypsin before resuspension. The A549 cells were divided into 6 groups, including a normal control (NC) group (normally cultured group), a group transfected with non-specific miRNA (Mock group), a miRNA-423-3p group (miRNA mimics group), a miRNA-423-3p inhibitor group (miRNA inhibitor group), a lncRNA MT1JP+miRNA-423-3p group (lncRNA MT1JP miRNA mimics group), and a lncRNA MT1JP+miRNA-423-3p blocker group (lncRNA MT1JP miRNA-423-3p inhibitor group).

### MTT assay for cell proliferation

Cells were adjusted to  $1 \times 10^5$  cells/mL, seeded into 96-well plates at 100  $\mu\text{L}$  per well, and cultured for 24 hours. After synchronizing with serum-free medium for 12 hours, each group of A549

cells was treated as described. Three parallel wells were prepared for each experiment, and the experiment was repeated 3 times independently. Cells were cultured at 37°C with 5%  $\text{CO}_2$  for 48 hours, the medium was refreshed, 10  $\mu\text{L}$  of 5  $\mu\text{g}/\text{mL}$  MTT was added to each well, and the plates were incubated once more at 37°C for 4 hours. Optical density at 570 nm was measured by a microplate reader to evaluate cell proliferation.

### Flow cytometry for apoptosis

Cells were digested in 0.25% trypsin (without EDTA) until they rounded up as observed under a microscope, then gently detached and dispersed into individual cells by pipetting, and then centrifuged at 1200 rpm for 5 minutes. The cell pellet was resuspended in Annexin V binding buffer, added with Annexin V-FITC and propidium iodide staining solution, and then incubated for 20 minutes at room temperature. Thereafter, the cells were placed on ice and were analyzed using flow cytometry.

### Colony formation assay

Cells were seeded into a 6-well cell culture plate at a density of 200 cells per well, and each group of cells was treated accordingly. After 10 days of culture, the supernatant was discarded, 4% paraformaldehyde was added to the wells, and the plate was incubated for another 25 minutes for fixation. The cells were then stained with 1% crystal violet for 30 minutes. The plates were photographed, and the number of colonies in each plate was counted. Three replicate wells were prepared for each group, and the experiment was repeated thrice.

### Scratch wound healing assay

Cells were seeded into 6-well cell plates at a density of  $8 \times 10^5$  cells per well and cultured with 2 mL of RPMI 1640 medium supplemented with 10% FBS for 24 hours to form a cell monolayer. A straight line was scratched into the monolayer with a 10  $\mu\text{L}$  pipette tip head. The cells were washed thrice with PBS, cultured with serum-free RPMI 1640 medium, and observed for 0, 24, and 48 hours under a reversed microscope with 100 $\times$  amplification. Photographs were taken at each time point, and the images were analyzed using ImageJ software. Three duplicate wells were prepared for each group, and the experiment was repeated thrice.

### Transwell assay

A Transwell chamber was placed in a 6-well plate. A total of  $1.5 \times 10^4$  cells in serum-free 1640 medium was added to the upper chamber, while 500  $\mu\text{L}$  of RPMI 1640 medium containing 10% FBS was added to the lower chamber. The cells were cultured in an incubator at 37°C with 5%  $\text{CO}_2$  for 24 hours. Thereafter, the Transwell chamber was removed, washed twice

with PBS, fixed with 4% paraformaldehyde at room temperature for 25 minutes, stained with 1% crystal violet for 30 minutes, and then washed with PBS. The chamber was dried in air and observed under a microscope (200×). For each sample, 5 views were randomly selected and photographed, and cells that had passed the membrane of the chamber were counted. Three duplicate wells were prepared for each group, and the experiment was repeated thrice.

### Luciferase activity assay

A549 cells were seeded into 48-well plates at a density of  $5 \times 10^4$  cells per well. At 70% confluence, plasmids for miRNA-NC, the miRNA-423-3p mimic, wildtype Bim (Bim-WT), and the Bim mutant (Bim-mut) were co-transfected with plasmids for galactose. Six hours after transfection, the transfection medium was replaced with DMEM containing 2% FBS, and the cells were cultured for another 48 hours. Luciferase activity was determined and compared using  $\beta$ -galactose as the internal control.

### RNA extraction and real-time polymerase chain reaction (RT-PCR) analysis

Total RNA was extracted from tissue samples and cells with a RNeasy RNA Mini Kit (QIAGEN, <http://www.qiagen.com>). To detect Bim, Bcl-2, and estimated glomerular filtration rate (EGFR) mRNA, first-strand cDNA was synthesized using AMV Reverse Transcriptase (Promega) with GAPDH as the internal control. The following primers were used for quantitative PCR: MT1JP forward: 5'-GCAAAGGGACGTCGGAGA-3', reverse: 5'-TCCAGGTTGTGAGGTTGTT-3', forward: 5'-AGCUCGGUCUGAGGCCUCAGU-3', reverse: 5'-UGAGGGGCCUCAGACCGAGCUUU-3'; Bim: forward: 5'-TGCAGTTGCTTCAGTACCCATAAT-3', reverse: 5'-ATCCCCGTGACTTCCCATATAAT-3'; Bcl-2: forward: 5'-TTCTTTGAGTTCGGTGGGGTC-3', reverse: 5'-TGCATATTTGTTGGGGCAGG-3'; EGFR: forward: 5'-CTAAGATCCCGTCCATCGCC-3', reverse: 5'-GGAGCCAGCACTTTGATCT-3'; GAPDH: forward: 5'-TGCACCACCAACTGCTTAGC-3', reverse: 5'-GGCATGGACTGTGGTCATGAG-3'.

### Western blotting for assessing the expression of related proteins

A549 cells were extracted with RIPA lysate, and 12.5% separation gel and 5% stacking gel were prepared. The protein was added to the comb hole for electrophoresis. Protein bands were transferred to a polyvinylidene difluoride (PVDF) membrane and incubated first with 5% skimmed milk powder for 1 hour and then with the corresponding primary antibodies (Bim, Bcl-2, EGFR, and GAPDH) at 4°C overnight. Next, the membrane was washed with TBST (Tris-buffered saline, 0.1%

Tween 20), incubated with the corresponding secondary antibodies, and visualized with enhanced chemiluminescence (ECL) agents. The images obtained were analyzed using ImageJ software to compare protein expression between groups.

### Statistical analysis

Statistical analysis was performed using SPSS 17.0 software. Measured data following a normal distribution are presented as mean  $\pm$  standard deviation (SD), and comparisons between groups were performed using one-way analysis of variance (ANOVA) and independent-samples *t*-test.  $P < 0.05$  was considered statistically significant.

## Results

### Clinical characteristics and data correlations

Hematoxylin and eosin staining revealed differences in cell infiltration and invasion among normal adjacent, stages I–II, and stages III–IV lung cancer tissues (Figure 1A). ISH assay indicated that the MT1JP expression of stages I–II and stages III–IV lung cancer tissues was significantly downregulated compared with that of adjacent normal tissues ( $P < 0.01$  or  $P < 0.001$ ; Figure 1B); by contrast, the miRNA-423-3p expression of stages I–II and stages III–IV lung cancer tissues was significantly upregulated compared with that of adjacent normal tissues ( $P < 0.01$  or  $P < 0.001$ ; Figure 1C). IHC assay revealed that the Bim protein expression of stages I–II and stages III–IV lung cancer tissues was significantly suppressed compared with that of adjacent normal tissues ( $P < 0.01$  or  $P < 0.001$ ; Figure 1D). Correlation analysis indicated that miRNA-423-3p was negatively correlated with MT1JP ( $r = -0.7763$ ,  $P = 0.000$ ; Figure 2A), Bim was negatively correlated with miRNA-423-3p ( $r = -0.8216$ ,  $P = 0.000$ ; Figure 2B), and Bim was positively correlated with MT1JP ( $r = 0.9654$ ,  $P = 0.000$ ; Figure 2C) in lung cancer tissues. Based on these results, we infer that MT1JP may be an anti-tumor factor in lung cancer.

### MT1JP and miRNA-423-3p genes expression of difference groups

By RT-PCR assay, the MT1JP gene expression of lncRNA+miRNA mimics and lncRNA+miRNA inhibitor groups were significantly up-regulation compared with that of NC group ( $P < 0.001$ , respectively, Figure 3); Meanwhile, compared with NC group, the miRNA-423-3p gene expression of miRNA mimics group was significantly up-regulation ( $P < 0.001$ . Figure 3), and the miRNA-423-3p gene expression of miRNA inhibitor and lncRNA+miRNA inhibitor group were significantly down-regulation ( $P < 0.001$ , respectively, Figure 3).

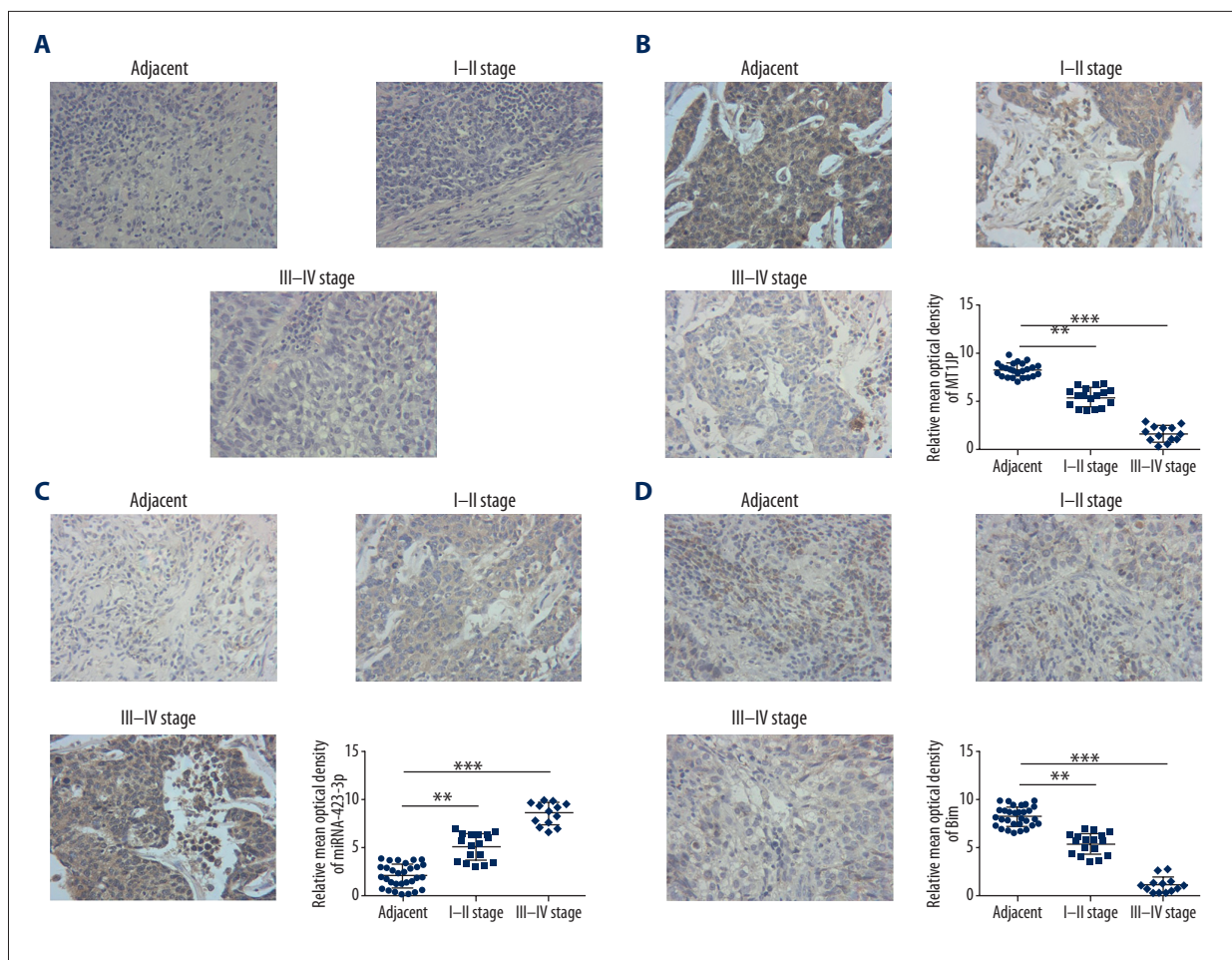


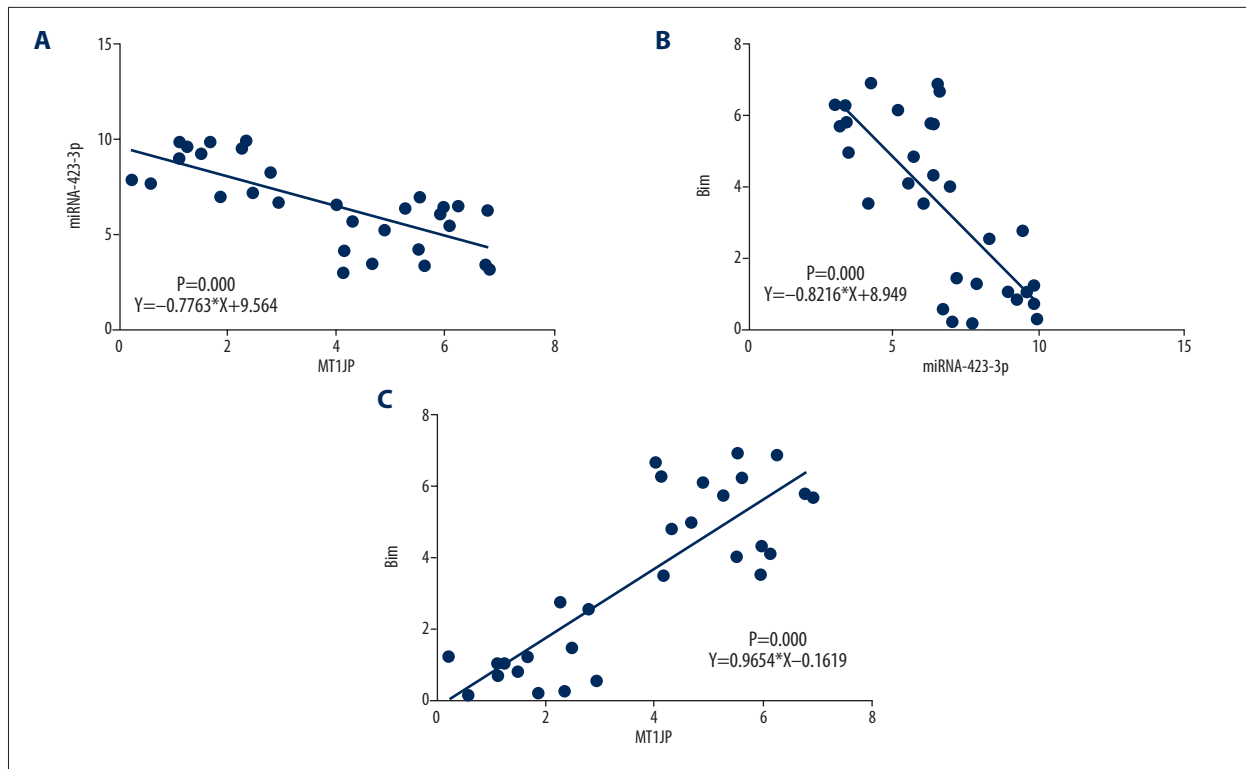
**Figure 1.** Clinical data. (A) The pathology of difference tissues by hematoxylin and eosin staining (200 $\times$ ). Adjacent – adjacent normal tissues; I-II stage – lung cancer tissues in I-II stage; III-IV stage – lung cancer tissues in III-IV stage. (B) MT1JP expression of difference tissues by ISH (200 $\times$ ). Adjacent – adjacent normal tissues; I-II stage – lung cancer tissues in I-II stage; III-IV stage – lung cancer tissues in III-IV stage; \*\*  $P < 0.01$ , \*\*\*  $P < 0.001$  versus adjacent tissue. (C) miRNA-423-3p expression of difference tissues by ISH (200 $\times$ ). Adjacent – adjacent normal tissues; I-II stage – lung cancer tissues in I-II stage; III-IV stage – lung cancer tissues in III-IV stage; \*\*  $P < 0.01$ , \*\*\*  $P < 0.001$  versus adjacent. (D) Bim protein expression by IHC (200 $\times$ ). Adjacent – adjacent normal tissues; I-II stage – lung cancer tissues in I-II stage; III-IV stage – lung cancer tissues in III-IV stage; \*\*  $P < 0.01$ , \*\*\*  $P < 0.001$  versus adjacent tissue. ISH – *in situ* hybridization; IHC – immunohistochemistry.

### MT1JP suppressed A549 cell proliferation and apoptosis

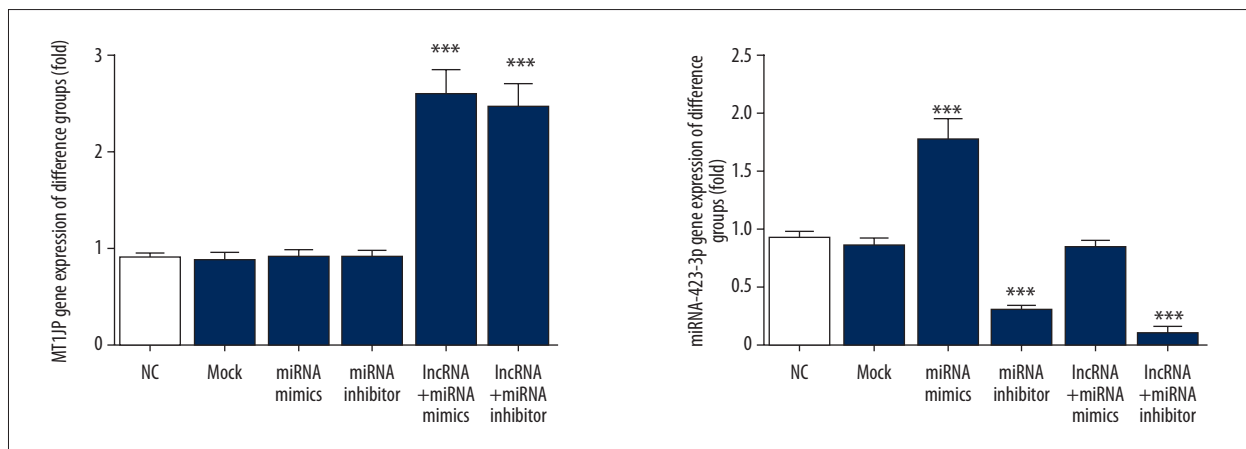
MTT assay revealed that the cell proliferation rate of the miRNA mimics group, which overexpressed miRNA-423-3p, was significantly upregulated compared with that of the NC group ( $P < 0.05$ ; Figure 4A). The cell proliferation rates of the miRNA-423-3p inhibitor and lncRNA+miRNA inhibitor groups were significantly downregulated compared with that of the NC group ( $P < 0.01$  or  $P < 0.001$ ; Figure 4A). In addition, the cell proliferation rate of the lncRNA+miRNA mimics group significantly increased compared with that of the miRNA mimics group ( $P < 0.01$ ; Figure 4A).

Colon formation assay demonstrated that the numbers of cell colonies and cells/field in the miRNA mimics group significantly increased compared with those in the NC group ( $P < 0.05$  or  $P < 0.01$ ; Figure 4B); by contrast, the numbers of cell colonies and cells/field of the miRNA inhibitor and lncRNA+miRNA inhibitor groups were significantly downregulated compared with those of the NC group ( $P < 0.05$ ,  $P < 0.01$ , or  $P < 0.001$ ; Figure 4B). In addition, the numbers of cell colonies and cells/field of the lncRNA+miRNA mimics group were significantly suppressed compared with those of the miRNA mimics group ( $P < 0.05$  or  $P < 0.01$ ; Figure 4B).

To evaluate the effect of MT1JP on A549 cell apoptosis, cell apoptosis in different groups was determined by flow



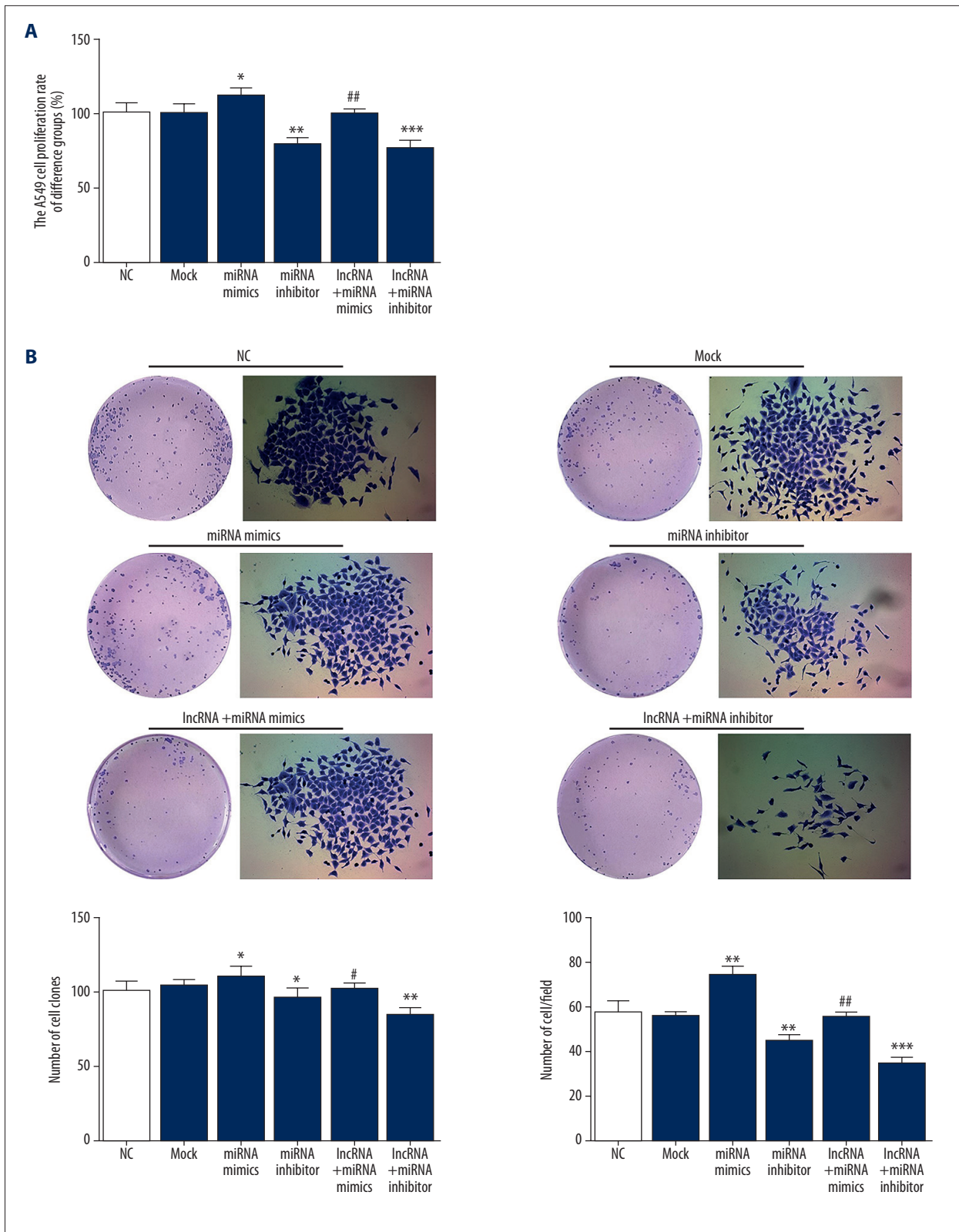
**Figure 2.** Analysis the correlation among clinical data. (A) Correlation between MT1JP and miRNA-423-3p;  $r=-0.7763$ ;  $P=0.000$ . (B) Correlation between Bim and miRNA-423-3p;  $r=-0.8216$ ;  $P=0.000$ . (C) Correlation between Bim and MT1JP;  $r=0.9654$ ;  $P=0.000$ .



**Figure 3.** MT1JP and miRNA-423-3p gene expression of difference groups. NC – normal control group; Mock – A549 cell transfected with empty vector; miRNA mimics – A549 cell transfected with miRNA-423-3p; miRNA inhibitor – A549 cell transfected with si-miRNA-423-3p; lncRNA+miRNA mimics – A549 cell transfected with MT1JP and miRNA-423-3p; \*\*\*  $P<0.001$  compared with NC group.

cytometry. Compared with that of the NC group, the cell apoptosis rate of the miRNA mimics group significantly decreased ( $P<0.01$ ; Figure 4C), whereas that in the miRNA inhibitor and lncRNA+miRNA inhibitor groups significantly increased ( $P<0.01$  or  $P<0.001$ ; Figure 4C). However, the cell apoptosis rate of the lncRNA+miRNA mimics group significantly increased compared

with that of the miRNA mimics group ( $P<0.01$ ; Figure 4C). The related data are shown in Figure 3.



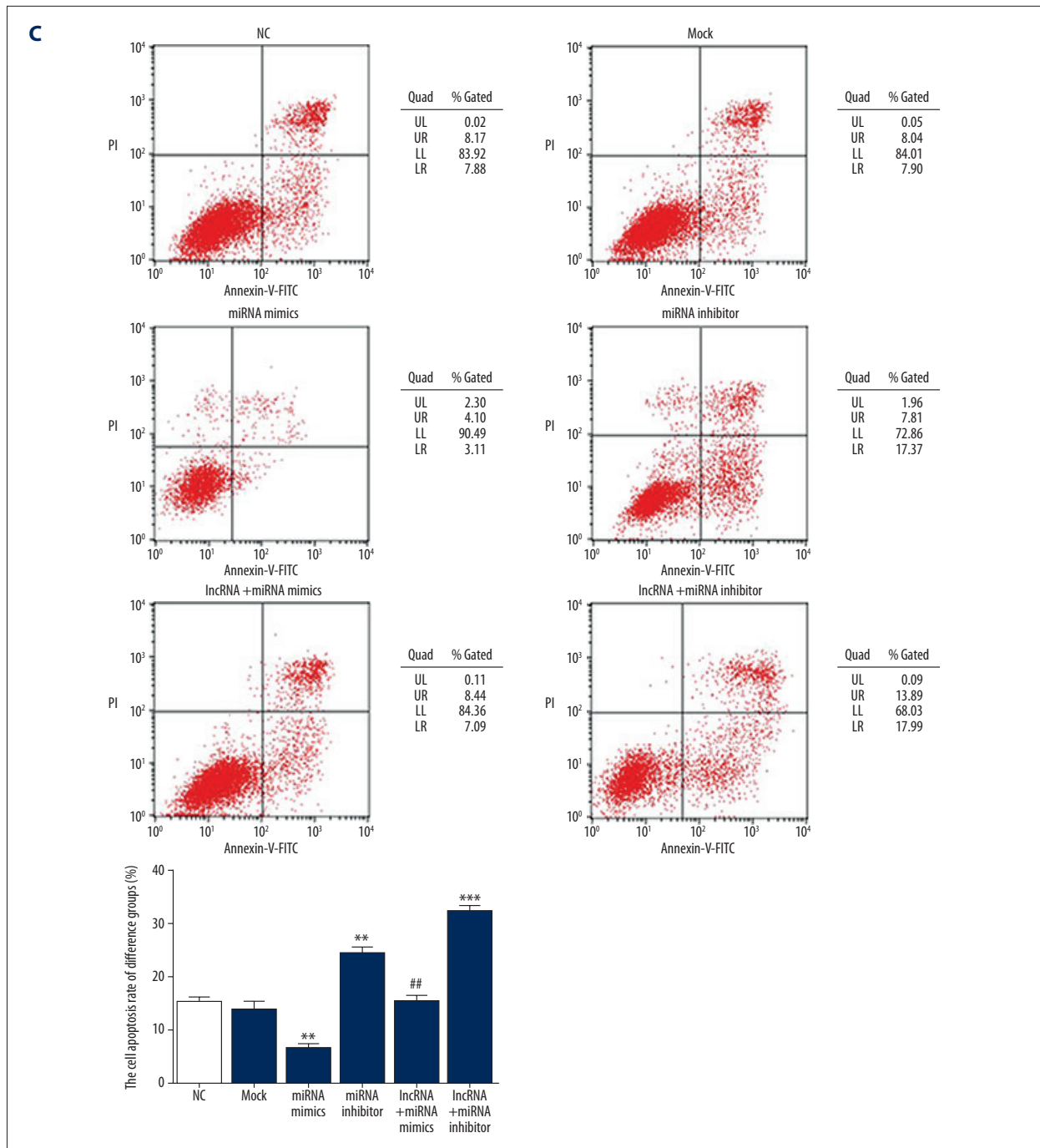


**Figure 4.** MT1JP affect A549 cell proliferation and apoptosis. **(A)** MT1JP affect A549 cell proliferation by MTT assay. NC – normal control group; Mock – A549 cell transfected with empty vector; miRNA mimics – A549 cell transfected with miRNA-423-3p; miRNA inhibitor – A549 cell transfected with si-miRNA-423-3p; lncRNA+miRNA mimics – A549 cell transfected with MT1JP and miRNA-423-3p; \*  $P < 0.05$ , \*\*  $P < 0.01$ , \*\*\*  $P < 0.001$  versus NC group; ##  $P < 0.01$  versus miRNA mimics. **(B)** MT1JP affect A549 cell proliferation by colony formation assay. NC – normal control group; Mock – A549 cell transfected with empty vector; miRNA mimics – A549 cell transfected with miRNA-423-3p; miRNA inhibitor – A549 cell transfected with si-miRNA-423-3p; lncRNA+miRNA mimics – A549 cell transfected with MT1JP and miRNA-423-3p; \*  $P < 0.05$ , \*\*  $P < 0.01$ , \*\*\*  $P < 0.001$  versus NC group; #  $P < 0.05$ , ##  $P < 0.01$  versus miRNA mimics. **(C)** MT1JP affect A549 cell apoptosis by flow cytometer. NC – normal control group; Mock – A549 cell transfected with empty vector; miRNA mimics – A549 cell transfected with miRNA-423-3p; miRNA inhibitor – A549 cell transfected with si-miRNA-423-3p; lncRNA+miRNA mimics – A549 cell transfected with MT1JP and miRNA-423-3p; \*  $P < 0.05$ , \*\*  $P < 0.01$ , \*\*\*  $P < 0.001$  versus NC group; ##  $P < 0.01$  versus miRNA mimics.



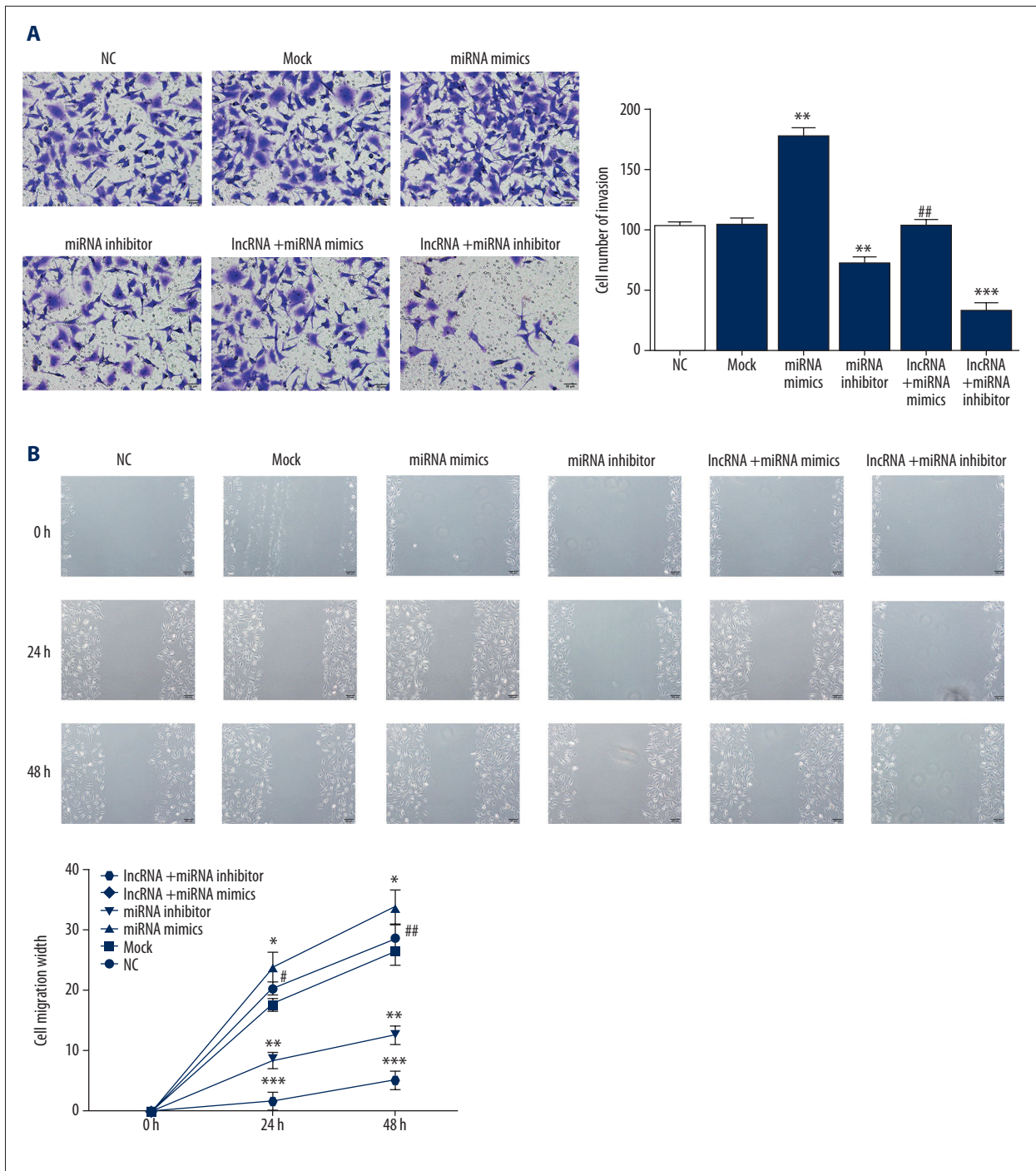


**Figure 5.** MT1JP affect A549 cell invasion and migration. **(A)** MT1JP affect cell number of invasion by Transwell assay; \*\*  $P < 0.01$ , \*\*\*  $P < 0.001$  versus NC group; ##  $P < 0.01$  versus miRNA mimics. **(B)** MT1JP affect A549 cell migration width by scratch wound healing assay; \*  $P < 0.05$ , \*\*  $P < 0.01$ , \*\*\*  $P < 0.001$  versus NC group; #  $P < 0.05$ , ##  $P < 0.01$  versus miRNA mimics. NC – normal control group.

### MT1JP inhibited A549 cell invasion and migration

To evaluate the effects of MT1JP on A549 cell invasion, the invading cell numbers of different groups were measured by Transwell assay. The invading cell number of the miRNA inhibitor group significantly increased compared with that of the NC group ( $P<0.01$ ; Figure 5A); by contrast, the invading cell numbers of the miRNA inhibitor and lncRNA+miRNA inhibitor groups significantly decreased compared with that of the NC group ( $P<0.01$  or  $P<0.001$ ; Figure 5A). In addition, the invading cell number of the lncRNA+miRNA mimics group was significantly downregulated compared with that of the miRNA mimic group ( $P<0.01$ ; Figure 5A).

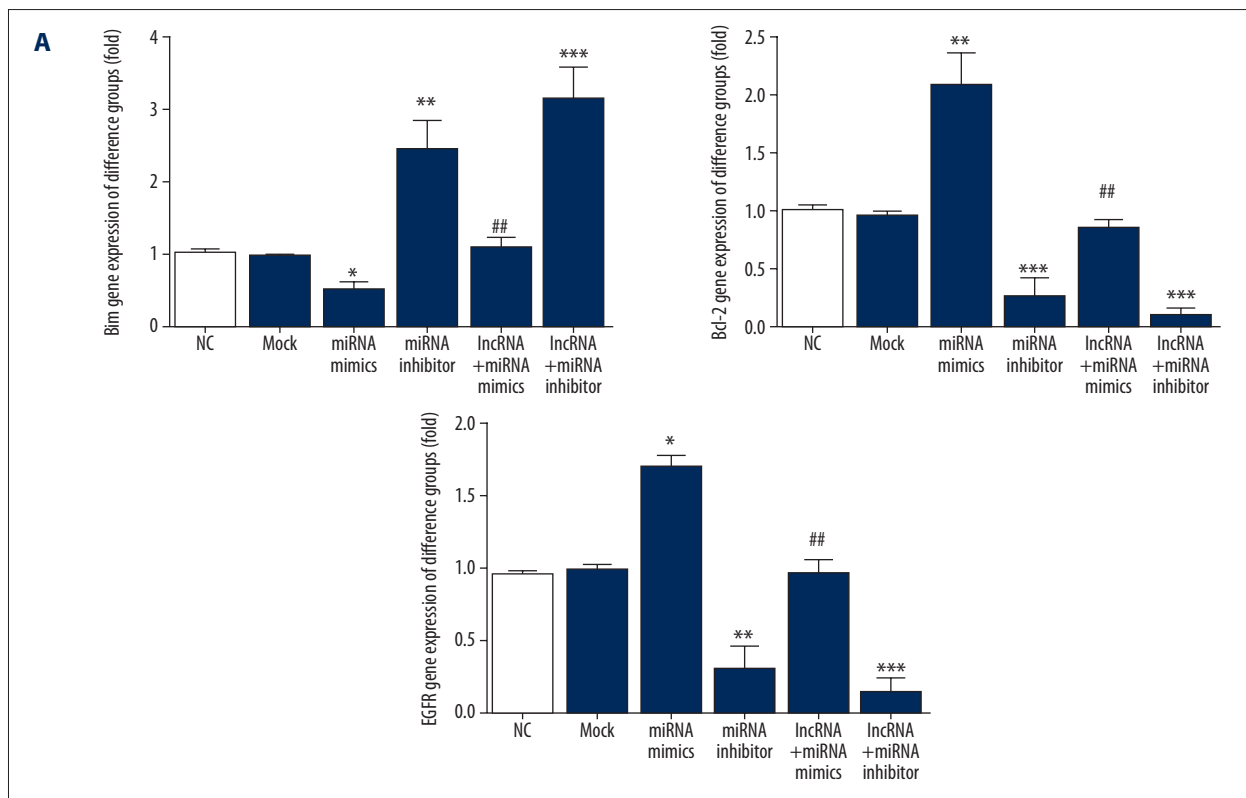
To evaluate the effects of MT1JP on A549 cell migration, the cell migration distance of different groups was measured by the scratch wound healing assay. The cell migration distance of the miRNA mimics group significantly increased compared with that of the NC group after 24 and 48 hours ( $P<0.05$ ; Figure 5B); by comparison, the cell migration distances of the miRNA inhibitor and lncRNA+miRNA inhibitor groups significantly decreased compared with that of NC group at the same time points ( $P<0.01$  or  $P<0.001$ ; Figure 5B). Finally, the cell migration distance of the lncRNA+miRNA mimics group was significantly upregulated compared with that of the miRNA mimics group after 24 and 48 hours ( $P<0.05$  or  $P<0.01$ ; Figure 5B). The relevant data are shown in Figure 5.

### MT1JP affects Bim relative gene and protein expressions

Compared with those in the NC group, Bim mRNA and protein expressions were significantly suppressed ( $P<0.05$ ), whereas Bcl-2 and EGFR mRNA and protein expressions were significantly increased ( $P<0.05$  or  $P<0.01$ ) in the miRNA mimics group. By contrast compared with those in the NC group, Bim mRNA and protein expressions were significantly increased ( $P<0.01$  or  $P<0.001$ ) whereas Bcl-2 and EGFR mRNA and protein expressions were significantly suppressed ( $P<0.01$  or  $P<0.001$ , respectively) in the miRNA inhibitor and lncRNA+miRNA inhibitor groups. Compared with those in the miRNA mimics group, Bim mRNA and protein expressions were significantly elevated and Bcl-2 and EGFR mRNA and proteins expressions were significantly suppressed ( $P<0.01$ ). The relevant data are shown in Figure 6.

### Bim is a direct target of miRNA-423-3p in A549 cells

Analysis of the correlations between miRNA-423-3p and Bim suggests the existence of a regulatory relationship between these molecules. Significant differences between miRNA-423-3p and NC ( $P<0.01$ ) were observed in Bim-WT, but no such differences were found in Bim-Mut (Figure 7A). Bim protein expression in different groups in Bim-WT and Bim-Mut determined by western blotting revealed significant suppression in the miRNA-423-3p groups compared with that in the NC



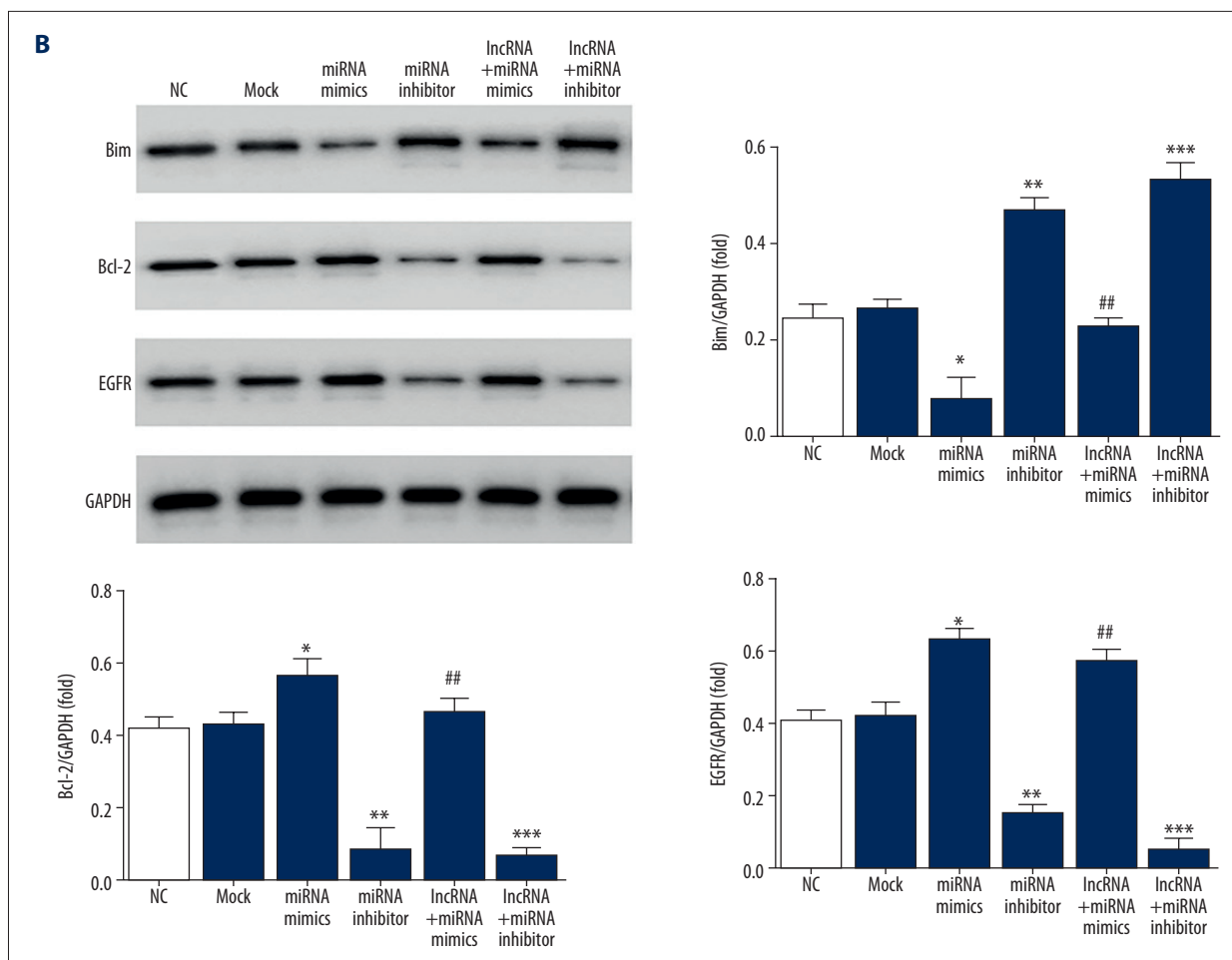


**Figure 6.** Relative mRNA and proteins expression. (A) Relative mRNA expression by RT-PCR; \*  $P < 0.05$ , \*\*  $P < 0.01$ , \*\*\*  $P < 0.001$  versus NC group; ##  $P < 0.01$  versus miRNA mimics. (B) Relative proteins expression by WB assay; \*  $P < 0.05$ , \*\*  $P < 0.01$ , \*\*\*  $P < 0.001$  versus NC group; ##  $P < 0.01$  versus miRNA mimics. RT-PCR – real-time polymerase chain reaction; WB – western blotting.

group in Bim-WT ( $P < 0.001$ ; Figure 7B). The relevant data are shown in Figure 7.

## Discussion

The Human Genome Project reveals that 98% of the sequences in the human genome do not encode proteins. Research has also found that these non-coding proteins may play important regulatory roles at multiple levels. A series of short-chain non-coding RNAs of about 18–25 nucleotides in length have been extensively studied, including miRNAs, siRNAs, and piRNAs. lncRNAs, another type of non-coding RNA, have drawn increased attention in recent years. Previous studies demonstrate that lncRNAs present a variety of biological functions in life activities, such as gene transcription and translation, cell differentiation and development, and genetics and epigenetics; they have also been shown to be involved in the development of tumors. Abnormal expression of lncRNAs has

been demonstrated to play a role in various tumors, such as breast cancer [17], bladder cancer [18], melanoma [19], liver cancer [20], and colorectal cancer [21]. Some lncRNAs seem to act as oncogenes. Wang et al., for example, demonstrated that the lncRNA MALAT1 significantly promotes the proliferation of gastric cancer cells by recruiting SF2/ASF; Yang et al. also found that the lncRNA GHET promotes the stability of Myc mRNA, thereby upregulating the expression of the proto-oncogene c-Myc and promoting the proliferation of gastric cancer cells [22,23]. Other researchers report that lncRNAs act as tumor suppressor genes. Han et al., for example, found in a study of gastric cancer that the lncRNA LEIGC inhibits epithelial–mesenchymal transition and plays a role in inhibiting tumor cell proliferation [24]. lncRNAs are also involved in the development of lung cancer, but their specific mechanism of action has not been fully elucidated. The results of this study showed that the MT1JP, miRNA-423-3p, and Bim are abnormally expressed in lung cancer tissues and correlated with the severity of lung cancer. Correlation analysis revealed that MT1JP is positively

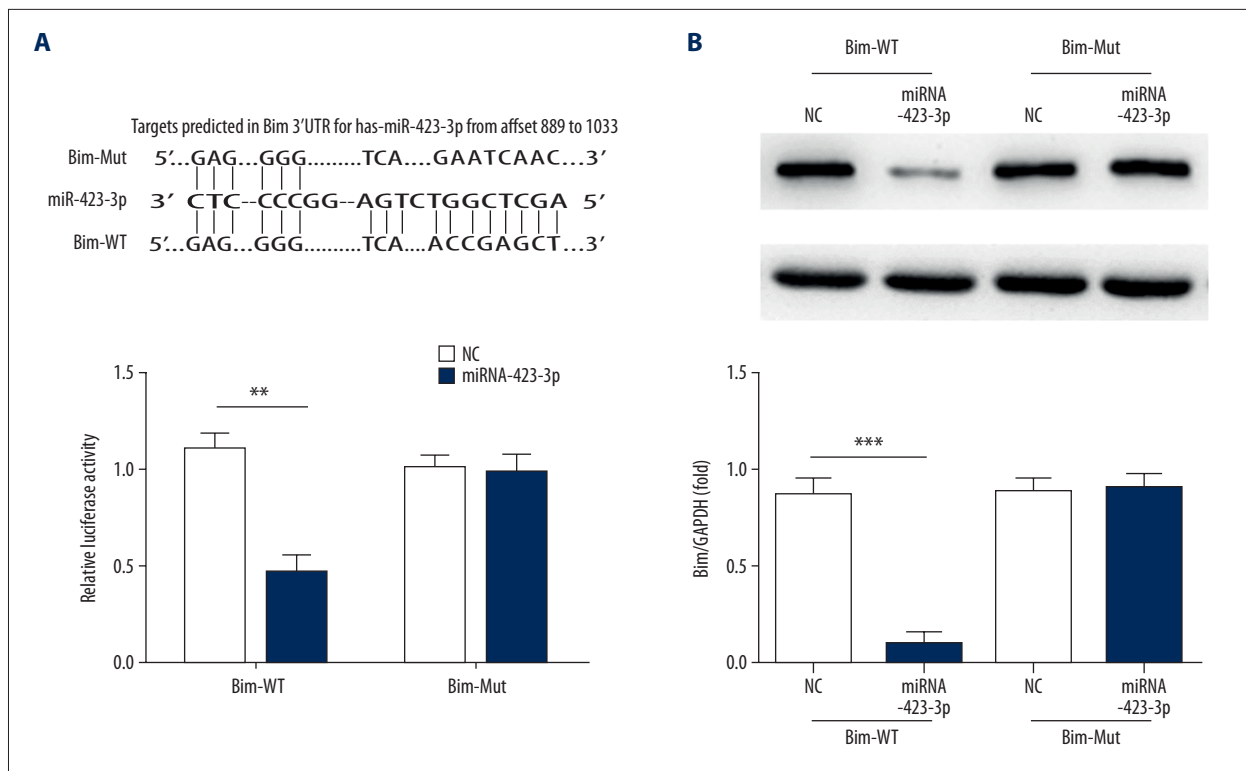


**Figure 7.** Correlation between miRNA-423-3p and Bim and the protein expression. **(A)** Analysis correlation between miRNA-423-3p and Bim by Luciferase activity assay; \*\*\*  $P < 0.001$  versus NC. **(B)** Bim protein expression by western blotting assay; \*\*\*  $P < 0.001$  versus NC. NC – normal control; WB – western blotting.

correlated with Bim and negatively correlated with miRNA-423-3p and that miRNA-423-3p is negatively correlated with Bim. Thus, we conclude that, during the development of lung cancer, MT1JP may regulate Bim by downregulating miRNA-423-3p. To verify the specific mechanism of MT1JP on NSCLC, we designed the corresponding cell experiments.

Cell experiments confirmed that the proliferation and migration of A549 cells are significantly inhibited and apoptosis is significantly increased after MT1JP transfection. However, when miRNA-423-3p was transfected into A549 cells with MT1JP, the proliferation, invasion, and migration of A549 cells were markedly restored. This result indicates that MT1JP inhibits the biological activity of NSCLC A549 cells and that such effect is closely related to a decrease in miRNA-423-3p levels. We further explored the anticancer mechanism of MT1JP using molecular biological methods.

Bim is a member of the BH3-only subfamily of the Bcl-2 family and is an important pro-apoptotic protein. Reportedly, a loss of Bim expression is associated with poor prognosis in a variety of tumors. Zhao et al. [25] found that Bim deficiency is closely associated with the pathogenesis of lung cancer. Maimaiti et al. [26] found that a loss of Bim expression is associated with poor prognosis in patients with breast cancer,

especially luminal A breast cancer. Zantl et al. [27] found that a loss of Bim expression is related to the development of chemotherapeutic resistance of renal cell carcinoma. These studies confirm that Bim is an important tumor suppressor. In the present study, bioinformatics analysis revealed that miRNA-423-3p has a binding site at the 3'-UTR of Bim mRNA, luciferase reporter assay confirmed that miRNA-423-3p can directly act on the Bim 3'-UTR, and WB showed that miRNA-423-3p effectively inhibits Bim protein expression. Based on these results, we hypothesized that MT1JP could inhibit the biological activity of A549 cells by downregulating miRNA-423-3p expression, which could lead to an increase in Bim expression.

The results of this study also revealed that Bcl-2 expression increased as Bim expression decreased. Bcl-2 is an anti-apoptotic protein that plays an important role in cell proliferation and apoptosis [28,29]. The results of this study indicated that decreased Bcl-2 expression may be a key factor leading to the inhibition of proliferation and increased apoptosis of A549 cells after MT1JP treatment. The main factor of increased apoptosis. EGFR is a member of the ErbB receptor family. Studies have shown that EGFR overexpression may be associated with tumor cell proliferation, invasion, metastasis, apoptosis, and angiogenesis in a variety of solid tumors and that EGFR mutations contribute to the malignant transformation of epithelial

cells [30]. In this study, EGFR protein expression was significantly inhibited as Bim protein expression increased, which may be the mechanism by which MT1JP inhibits the invasion and migration of A549 cells.

## References:

- Hong QY, Wu GM, Qian GS et al: Prevention and management of lung cancer in China. *Cancer*, 2015; 121(Suppl. 17): 3080–88
- Global Burden of Disease Cancer Collaboration, Fitzmaurice C, Akinyemiju TF, Al Lami FH, et al: Global, regional, and national cancer incidence, mortality, years of life lost, years lived with disability, and disability-adjusted life-years for 29 cancer groups, 1990 to 2016: A systematic analysis for the global burden of disease study. *JAMA Oncol*, 2018; 4(11): 1553–68
- Bouillet P, Zhang LC, Huang DC et al: Gene structure alternative splicing, and chromosomal localization of pro-apoptotic Bcl-2 relative Bim. *Mamm Genome*, 2001; 12(2): 163–68
- Faber AC, Ebi H, Costa C et al: Apoptosis in targeted therapy responses: The role of BIM. *Adv Pharmacol*, 2012; 65: 519–42
- Ng KP, Hillmer AM, Chuah CT et al: A common BIM deletion polymorphism mediates intrinsic resistance and inferior responses to tyrosine kinase inhibitors in cancer. *Nat Med*, 2012; 18(4): 521–28
- Nakagawa T, Takeuchi S, Yamada T et al: EGFR-TKI resistance due to BIM polymorphism can be circumvented in combination with HDAC inhibition. *Cancer Res*, 2013; 73(8): 2428–34
- Isobe K, Hata Y, Tochigi N et al: Clinical significance of BIM deletion polymorphism in non-small-cell lung cancer with epidermal growth factor receptor mutation. *J Thorac Oncol*, 2014; 9(4): 483–87
- Chandra Gupta S, Nandan Tripathi Y: Potential of long non-coding RNAs in cancer patients: From biomarkers to therapeutic targets. *Int J Cancer*, 2017; 140(9): 1955–67
- Liu L, Yue H, Liu Q et al: LncRNA MT1JP functions as a tumor suppressor by interacting with TIAR to modulate the p53 pathway. *Oncotarget*, 2016; 7(13): 15787–800
- Komarova EA, Krivokrysenko V, Wang K et al: p53 is a suppressor of inflammatory response in mice. *FASEB J*, 2005; 19(8): 1030–32
- Xu Y, Zhang G, Zou C et al: LncRNA MT1JP suppresses gastric cancer cell proliferation and migration through MT1JP/MiR-214-3p/RUNX3 axis. *Cell Physiol Biochem*, 2018; 46(6): 2445–59
- Rui X, Xu Y, Huang Y et al: LncRNA DLG1-AS1 promotes cell proliferation by competitively binding with miR-107 and up-regulating ZHX1 expression in cervical cancer. *Cell Physiol Biochem*, 2018; 49(5): 1792–803
- Wang YG, Liu J, Shi M et al: LncRNA DGCR5 represses the development of hepatocellular carcinoma by targeting the miR-346/KLF14 axis. *J Cell Physiol*, 2018; 234(1): 572–80
- Brigant B, Metzinger-Le Meuth V, Massy ZA et al: Serum microRNAs are altered in various stages of chronic kidney disease: A preliminary study. *Clin Kidney J*, 2017; 10(4): 578
- Papoutsidakis N, Ahmad T, Jacoby D: Our unquenched thirst to improve prediction of heart failure risk: From jugular venous distention to microRNAs. *J Heart Lung Transplant*, 2017; 36(6): 607–8
- Alrob OA, Khatib S, Naser SA: MicroRNAs 33, 122 and 208: A potential novel targets in the treatment of obesity, diabetes, and heart-related diseases. *J Physiol Biochem*, 2017; 73(2): 307–14
- Gupta RA, Shah N, Wang KC et al: Long non-coding RAN HOTAIR reprograms chromatin state to promote cancer metastasis. *Nature*, 2010; 464(7291): 1071–76
- Zhu Y, Yu M, Li Z et al: LncRAN, a newly identified long noncoding RNA, enhances human bladder tumor growth, invasion, and survival. *Urology*, 2011; 77(2): 510.e1–5
- Khaïtan D, Dinger ME, Mazar J et al: The melanoma-upregulated long non-coding RNA SPRY4-IT1 modulates apoptosis and invasion. *Cancer Res*, 2011; 71(11): 3852–62
- Yuan SX, Yang F, Yang Y et al: Long noncoding RNA associated with microvascular invasion in hepatocellular carcinoma promotes angiogenesis and serves as a predictor for hepatocellular carcinoma patients' poor recurrence-free survival after hepatectomy. *Hepatology*, 2012; 56(6): 2231–41
- Kogo R, Shimamura T, Mimori K et al: Long noncoding RNA HOTAIR regulates polycomb-dependent chromatin modification and is associated with poor prognosis in colorectal cancers. *Cancer Res*, 2011; 71(20): 6320–26
- Yang F, Xue X, Zheng L et al: Long non-coding RNA GHET1 promotes gastric carcinoma cell proliferation by increasing c-Myc mRNA stability. *FEBS J*, 2014; 281(3): 802–13
- Wang J, Su L, Chen X et al: MALAT1 promotes cell proliferation in gastric cancer by recruiting SF2/ASF. *Biomed Pharmacother*, 2014; 68(5): 557–64
- Han Y, Ye J, Wu D et al: LEIGC long non-coding RNA acts as a tumor suppressor in gastric carcinoma by inhibiting the epithelial-to-mesenchymal transition. *BMC Cancer*, 2014; 14: 932
- Zhao M, Zhang Y, Cai W et al: The Bim deletion polymorphism clinical profile and its relationship with tyrosine kinase inhibitor resistance in Chinese patients with non-small cell lung cancer. *Cancer*, 2014; 120(15): 2299–307
- Maimaiti Y, Dong L, Aili A et al: Bim may be a poor prognostic biomarker in breast cancer patients especially in those with luminal A tumors. *Cancer Biomark*, 2017; 19(4): 411–18
- Zantl N, Weirich G, Zall H et al: Frequent loss of expression of the pro-apoptotic protein Bim in renal cell carcinoma: Evidence for contribution to apoptosis resistance. *Oncogene*, 2007; 26(49): 7038–48
- Grabow S, Kueh AJ, Ke F et al: Subtle changes in the levels of BCL-2 proteins cause severe craniofacial abnormalities. *Cell Rep*, 2018; 24(12): 3285–95
- Zeng M, Huang C, Zheng H et al: Effects of ghrelin on iNOS-derived NO promoted LPS-induced pulmonary alveolar epithelial A549 cells apoptosis. *Cell Physiol Biochem*, 2018; 49(5): 1840–55
- Joseph SR, Gaffney D, Barry R et al: An *ex vivo* human tumour assay reveals distinct patterns of EGFR trafficking in squamous cell carcinoma correlating to therapeutic outcomes. *J Invest Dermatol*, 2019; 139(1): 213–23

## Conclusions

In summary, MT1JP can effectively inhibit the biological activity (i.e., proliferation, invasion, and migration) of NSCLC A549 cells, and this effect may be largely attributed to the decrease in the expression of miRNA-423-3p and the upregulation of Bim, the target of miRNA-423-3p.